



In situ forming hydrogel of natural polysaccharides through Schiff base reaction for soft tissue adhesive and hemostasis

Jia Liu^{a,b,1}, Jun Li^{a,1}, Fan Yu^{c,1}, Ya-xin Zhao^c, Xiu-mei Mo^{c,*}, Jian-feng Pan^{a,*}

^a Department of Orthopedics, Shanghai Tenth People's Hospital affiliated to Tongji University, 301 Yanchang Road, Shanghai 200072, China

^b Department of Orthopedics, Shidong Hospital of Yangpu District, 999 Shiguang Road, Shanghai 200438, China

^c State Key Laboratory for Modification of Chemical Fibers and Polymer Materials, College of Chemistry, Chemical Engineering and Biotechnology, Donghua University, 2999 North Renmin Road, Shanghai 201620, China

ARTICLE INFO

Article history:

Received 8 August 2019

Received in revised form 21 December 2019

Accepted 2 January 2020

Available online 7 January 2020

Keywords:

Aldehyde hydroxyethyl starch

Amino carboxymethyl chitosan

Tunable properties

Hydrogel

Schiff base reaction

Soft tissue adhesive

Hemostasis

ABSTRACT

In this study, a novel injectable hydrogel with biocompatibility and biodegradability through Schiff base reaction was prepared for soft tissue adhesive and hemostasis. Aldehyde hydroxyethyl starch (AHES) was prepared by oxidizing hydroxyethyl starch to get aldehyde groups. Amino carboxymethyl chitosan (ACC) was prepared by grafting ethylenediamine onto carboxymethyl chitosan to get more amino groups. Two-component AHES/ACC hydrogel was formed through Schiff base reaction between aldehyde and amino groups. By changing the reaction conditions various contents of aldehyde and amino group were achieved. The properties of AHES/ACC hydrogel were tunable including gelation time, swelling ratio, degradation and mechanical tensile by varying the content of aldehyde and amino groups. Then biocompatibility measurements showed that AHES/ACC hydrogels supported cell viability and proliferation in vitro and exhibited good biodegradability and biocompatibility in vivo. AHES/ACC hydrogel also had effective hemostatic ability. Thus, this study provides a strategy for the design and fabrication of fast in situ forming hydrogels. Through Schiff base reaction in situ forming hydrogel derived from natural polysaccharides can be modulated and prepared for soft tissue adhesive, hemostasis or other biomedical applications in future.

© 2020 Elsevier B.V. All rights reserved.

1. Introduction

Traumatic injuries are common events in daily life, among which large-area tissue defects and wounds are especially difficult to deal with during the process of medical treatments. They not only require the wound to close in time, but also require the effective hemostasis of wound. This highlights the necessity of exploring and developing novel soft tissue adhesive and wound hemostatic agents. Recently, in situ forming hydrogels have attracted great attention in tissue engineering and regenerative medicine. Hydrogels consist of crosslinked hydrophilic polymers that can swell in water with 3D network structure [1]. The hydrophilic groups in the hydrogel (such as -OH, -COOH, etc.) are capable of diffusing water molecules into the interior of the hydrogel, thereby retaining a large amount of water in the hydrogel network structure. The volume of water absorbed by hydrogels may range from 10% to thousands of times of its own volume. This property of the hydrogel makes it structurally resemble natural soft tissues and

extracellular matrices more than any other scaffolds. Generally, hydrogels exhibit good permeability and biocompatibility. Water and other water-soluble small molecules such as oxygen and nutrients can diffuse freely inside and outside the hydrogels [2,3]. This makes them promising scaffolds in tissue engineering for encapsulating bioactive molecules, delivering specific biofactor signals and supporting cell proliferation and differentiation [4–6].

According to the crosslinking mechanism of 3D network structure, hydrogels can be classified into physical crosslinking gels and chemical crosslinking gels. In physically crosslinked gels, no new bond is formed and the crosslinked network structure is formed by polymer chain entanglement, crystallization point and other physical interactions (such as ionic bond, van der Waals force, hydrogen bond, etc.). A major disadvantage of physical crosslinking gels is that they are hard to be customized and modulated to satisfy specific needs. Some of them are inhomogeneous when the conditions are changed [7]. In chemically crosslinked gels, new covalent bonds are formed between different polymer chains and a three-dimensional network structure is formed in a permanently irreversible manner [8]. Chemical crosslinked hydrogels can be formed by covalent crosslinking, chemical conjugation, polyesterification, copolymerization or polycondensation. To

* Corresponding authors.

E-mail addresses: xmm@dhu.edu.cn (X. Mo), pansmith@163.com (J. Pan).

¹ Jia Liu, Jun Li and Fan Yu contributed equally to this work.

date, various types of natural polymers have been used in the manufacture of hydrogel scaffolds due to their good biocompatibility, inherent biodegradability and important biological characteristics.

Natural polysaccharides, as major type of natural polymers, have attracted great attention in tissue engineering and regenerative medicine. They can be chemically modified and grafted with various functional groups such as acrylate, thiol, furyl and amine for chemical crosslinking [9–11]. Among them, chitosan and starch have been fabricated by some professors as various hydrogels with excellent biocompatibility, biodegradability and non-toxicity to control delivery of biotherapeutics and facilitate tissue regeneration [12–14]. In their papers, chitosan and starch were modified to prepare in situ forming hydrogels through Schiff base reaction and the influence of constituent ratio on physicochemical properties of resultant hydrogels was examined [15,16]. Apart from the constituent ratio, experimental parameters also have an important influence on the physicochemical properties of hydrogels including the degree of oxidation and amination. Thus, in this study in situ forming hydrogel of chitosan and starch was prepared and controlled by varying the degree of oxidation and amination.

Chitosan is obtained by deacetylation of chitin, which is widely available in the shells of marine crustacean shrimps, crabs and insects. It is linear 2-amino-deoxy- β -D-glucose linked by β -(1,4) glycosidic bond. Due to its good biocompatibility, biodegradability and certain antibacterial properties, it has a wide range of potential applications in biomedical engineering. But insolubility of chitosan in water and complete dissolution only in solution with pH values below 6 have prevented its widely exploitation in tissue repair and regeneration. Chemical modification of chitosan is a promising way to get rid of these limitations and different derivatives of chitosan have been synthesized by experts and scholars to widen the application of chitosan in tissue engineering. Carboxymethyl chitosan (CC), as one of the water dissoluble derivatives of chitosan, overcomes the shortcoming of insolubility. Compared with its parent polymer chitosan, CC has excellent biocompatibility, improved biodegradability, enhanced antibacterial activity and moisture retention capacity [17]. This contributes to the widespread use of this biopolymer in the fields of bone [18], cartilage [19], nerve [20] tissue engineering and wound healing. Hydroxyethyl starch (HES) is a synthetic colloid that has been approved and used for fluid therapy in the perioperative surgical patients for decades [21]. Despite increasing attention has been paid to the adverse effects of HES on mortality, major infectious complications and acute kidney injury, there is currently insufficient data to confirm it [22]. Due to excellent biocompatibility, low immunogenicity, inherent biodegradability and the abundance of functional groups available for chemical modification, HES has extensively been investigated for application in tissue engineering [23,24].

The purpose of this study was to fabricate an in situ forming hydrogel composed of aldehyde hydroxyethyl starch and amino carboxymethyl chitosan for soft tissue adhesive and hemostasis. The main components of this injectable hydrogel system are derived from polysaccharides with biocompatibility, biodegradability and non-toxicity. Aldehyde hydroxyethyl starch (AHES) was prepared by oxidizing hydroxyethyl starch with sodium periodate to get aldehyde groups. Amino carboxymethyl chitosan (ACC) was prepared by modifying carboxymethyl chitosan with ethylenediamine to get amino groups. Various contents of aldehyde and amino group were achieved by changing the reaction conditions, that were different molar ratio of sodium periodate to hydroxyethyl starch ($n(\text{NaIO}_4)/n(\text{H})$) and ethylenediamine to carboxymethyl chitosan ($n(\text{ED})/n(\text{COOH})$). Fourier Transform Infrared Spectroscopy was used to confirm structural characteristics. Two-component AHES/ACC hydrogels with various contents of aldehyde and amino group were formed through Schiff base reaction. The properties of AHES/ACC hydrogel were investigated including gelation time, swelling ratio, degradation and mechanical tensile. The results showed that these properties could be modulated by varying the content of aldehyde and amino groups. According to the specific requirements of biomedical applications, the injectable AHES/ACC

hydrogel could be manipulated as a promising scaffold. Furthermore, cell cytotoxicity of AHES/ACC hydrogel in vitro was evaluated by culturing bone marrow mesenchymal stem cells (BMSCs) with hydrogels. The hemostasis efficacy of AHES/ACC hydrogel was assessed by a SD rat liver model and vital organs were observed to evaluate biocompatibility of AHES/ACC hydrogel in vivo at different time points. The results showed that AHES/ACC hydrogels supported cell viability and proliferation in vitro and exhibited effective hemostatic ability and biocompatibility in vivo. Thus, AHES/ACC hydrogels are potential for future use as tissue adhesives and hemostatic wound dressings in clinic.

2. Materials and methods

2.1. Materials

Carboxymethyl chitosan (molecular weight of 200 kDa) with a substitution degree of 90% and a deacetylation degree of 82% was purchased from Bangcheng Chemical Co., Ltd. (Shanghai, China). Hydroxyethyl starch (molecular weight of 130 kDa) with a substitution degree of 40%, sodium periodate, ethylenediamine (ED) and chloral hydrate were purchased from Sigma-Aldrich (St Louis, MO, USA). 1-Ethyl-3-(3-dimethyl laminopropyl) carbodiimide hydrochloride (EDC) was purchased from GL Biochem Corporation (Shanghai, China). Fibrin glue was purchased from Bioseal Biotech Corporation (Guangzhou, China). Fetal bovine serum (FBS), Dulbecco's modified Eagle's medium (DMEM), phosphate buffered saline (PBS) and other reagents were purchased from Gibco Life Technologies Corporation (Carlsbad, CA, USA) to prepare complete medium for cell culture. CCK-8 was purchased from Dojindo Corporation (Kumamoto, Japan).

2.2. Preparation of aldehyde hydroxyethyl starch

Hydroxyethyl starch was oxidized by sodium periodate to get aldehyde hydroxyethyl starch (AHES) with different degree of oxidation according to the previously described method [25]. Firstly, 10% (w/v) hydroxyethyl starch solution (100 mL) was prepared by dissolved hydroxyethyl starch in deionized water. 10% (w/v) sodium periodate solution was prepared by dissolved NaIO_4 in deionized water. Then different amounts of NaIO_4 solution was added dropwise into hydroxyethyl starch solution and stirred at room temperature for 4 h. The reaction process was shielded from light. After that, 2 mL of ethylene glycol was added into the reaction system to terminate the reaction. The product was loaded into a dialysis bag ($\text{MW} = 3500$) and dialyzed in deionized water for 3 days with several changes of water till the dialyzate was both periodate and ethylene glycol free. Then the reaction product was frozen at -80°C and lyophilized in an ultra-low temperature freeze dryer to obtain AHES. AHES with different content of aldehyde group was achieved by varying the amount of oxidizing agent during the oxidation reaction.

2.3. Structural characterization and measurement of aldehyde group content

The prepared AHES and unoxidized hydroxyethyl starch were structurally characterized by Fourier Transform Infrared Spectroscopy (FTIR-ATR). The aldehyde group content (AGC) of AHES was determined by hydroxylamine hydrochloride titration method. AGC was defined as the molar ratio of oxidized-opened aldose unit to total hydroxyethyl starch glucopyranose ring monomer unit. Dialdehyde groups of oxidized-opened aldose unit reacted with hydroxylamine hydrochloride to release hydrochloric acid, which was equivalent to aldehyde group. The reaction is as follows: $\text{HES}-(\text{CHO})_n + \text{H}_2\text{N}-\text{OH} \cdot \text{HCl} = \text{HES}-(\text{CH} = \text{N}-\text{OH})_n + \text{H}_2\text{O} + \text{HCl}$. Through calculating the amount of released HCl, the amount of aldehyde groups can be calculated. Briefly, AHES sample (0.1000 g) was mixed with 5.0 mL of hydroxylamine hydrochloride solution and 5.0 mL of absolute ethanol. The mixture was

slowly heated and refluxed for 40 min, then cooled to room temperature and titrated with hydrochloric acid. The consumption volume of hydrochloric acid was recorded when the color changed to yellowish green. The blank test without AHES was performed in the same procedure.

The aldehyde group content of AHES was calculated by: aldehyde group content = $(V_0 - V_1) \cdot C \cdot M / 2W$, where V_0 is the volume of HCl consumed for the blank test (L), V_1 is the volume of HCl consumed for the sample test (L), C is the concentration of HCl solution (mol/L), M is the molecular weight of a monomer unit of hydroxyethyl starch, and W is the weight of the AHES sample added in the hydroxylamine hydrochloride solution.

The oxidation efficiency was calculated by: oxidation efficiency = actual aldehyde group content/theoretical aldehyde group content.

2.4. Preparation of amino carboxymethyl chitosan

The preparation of amino carboxymethyl chitosan (ACC) was inspired by the method of synthesizing amino gelatin described in the previous study [26]. Firstly, 200 mL sodium dihydrogen phosphate solution (0.1 mol/L) was prepared and 5 g of carboxymethyl chitosan (CC) was added into the solution. The CC was completely dissolved overnight by a magnetic stirrer. After that ethylenediamine (ED) was added. The pH value of solution was adjusted to 5.0 by adding hydrochloric acid and then EDC was added into the solution. The molar ratio of EDC to carboxyl groups (COOH) on CC chains was 2:1. The molar ratio of ED to COOH was 5, 10, 20 and 30 to 1 so as to obtain products with various degree of chemical modification. The reaction process was going on for 6 h at 37 °C by stirring with a magnetic stirrer. After that, the reaction product was loaded into a dialysis bag (MW = 3500) and dialyzed in deionized water for 3 days till the dialyzate was both ethylenediamine and EDC free. Then the reaction product was frozen at −80 °C and lyophilized in an ultra-low temperature freeze dryer to obtain ACC. ACC with different content of amino group was achieved by varying the amount of ethylenediamine during the amination reaction.

2.5. Structural characterization and measurement of amino group content

The prepared ACC and CC were structurally characterized by Fourier Transform Infrared Spectroscopy (FTIR-ATR). The amino group content of ACC was determined by reacting with trinitrobenzenesulfonic acid (TNBS) according to the previous method [26]. Briefly, ACC was dissolved in PBS solution to obtain ACC solution with the concentration of 5% (pH = 7.4). 1 mL of ACC solution was mixed with 1 mL of 4% sodium bicarbonate solution and 1 mL of 0.1% 2,4,6-TNBS solution. The mixture was shielded from light and incubated at 40 °C for 2 h. After that, the absorbance of the solution was measured at 415 nm using a microplate reader. Then, β-alanine solution with gradient concentration was performed in the same procedure and a standard curve was obtained to show the relationship between the absorbance and the concentration for the β-alanine solution. According to this, the amino content of ACC was calculated. In addition, the percentage of carboxyl groups converted into amino groups could be calculated based on the change of amino group content before and after chemical modification. The formula is as follow:

Carboxyl modification efficiency = $(A_a - A_b)/C$.

where A_a is the amino content of CC after chemical modification, A_b is the amino content of CC before chemical modification, C is the carboxyl content of CC before chemical modification.

After chemical modification, flow property of CC and ACC solution was tested using a vial tilting approach. CC and ACC were firstly formulated into 5% (w/v) solution in a vial and placed at

4 °C overnight. Then, the two sample solutions were incubated in a water bath with a temperature increment of 1 °C per time. After the temperature rose to a fixed value, the vial was taken out and observed obliquely. Until a certain temperature, the internal solution of the vial appeared to flow. The temperature at that time was regarded as the sol-gel transition temperature.

2.6. Preparation of AHES/ACC hydrogel and measurement of gelation time

AHES with different aldehyde content was dissolved to prepare 10% AHES solution and ACC with different amino content was dissolved to get 5% ACC solution. AHES solution and ACC solution was respectively filled in a 5 mL syringe. These two syringes were mounted with a Y-type syringe needle together. By pushing the double hybrid syringes, the mixed solution of AHES and ACC was extruded from the Y-type syringe needle. As the Schiff base reaction progressed in the hydrogel precursor solution, AHES and ACC crosslinked to form AHES/ACC hydrogel.

0.5 mL of 10% AHES solution was injected into a small glass bottle with a magnetic rotor. The rotor was stabilized at the speed of 1 r/s by a magnetic stirrer. Then 0.5 mL of 5% ACC solution was added into the small glass bottle. At this point, the time started to count. When the rotor stopped rotating, the total duration of time was recorded, which was the gelation time of AHES/ACC hydrogel. The gelation time was measured between AHES with different aldehyde group content (molar ratio of sodium periodate to hydroxyethyl starch unit) and ACC with different amino group content (molar ratio of ED to carboxyl group in CC). Three parallel duplicates were measured for each sample and statistical analysis was performed.

2.7. Equilibrium swelling properties of AHES/ACC hydrogel

In this experiment, three parallel duplicates of AHES/ACC hydrogel were prepared and completely swelled in deionized water at 37 °C to reach the equilibrium swelling state. The excess moisture on the surface of swollen hydrogel was absorbed by a filter paper. The swollen quality of hydrogel (W_s) after completely swelling was accurately weighed. Then the hydrogel was frozen at −80 °C and lyophilized in an ultra-low temperature freeze dryer. The dry quality of hydrogel (W_d) after lyophilization was accurately weighed. The swelling ratio (SR) of AHES/ACC hydrogel was calculated by the formula: $SR = (W_s - W_d) / W_d$. The equilibrium water content (EWC) of AHES/ACC hydrogel was calculated by the formula: $EWC = (W_s - W_d) / W_s \times 100\%$. Three parallel specimens were measured for each group and statistical analysis was performed.

2.8. In vitro degradation properties of AHES/ACC hydrogel

The in vitro degradation properties of hydrogels were examined using the weight loss method. First, the mass of each hydrogel sample was accurately weighed and recorded as (W_0). The weighed hydrogel sample was immersed in 20 mL of PBS and placed in an incubator shaker at 37 °C for in vitro degradation. After different time interval, the degraded hydrogel sample was taken out and wiped off with a filter paper. The residual mass of each hydrogel sample was accurately weighed and recorded as (W_1). The residual mass percentage of the hydrogel after degradation with time (Weight remaining %) was calculated by the formula: $\text{Weight remaining \%} = W_1 / W_0 \times 100\%$. W_1 is the mass of the hydrogel after degradation at a specific time point. W_0 is the initial mass of the hydrogel. All samples were tested in triplicate.

2.9. Mechanical tensile test of AHES/ACC hydrogel

In this experiment, the mechanical properties of AHES/ACC hydrogel were determined by stretching the pigskin according to the reported method [27]. After the pigskins were cleaned, they were

cut into pieces of 1 cm in width and 3 cm in length. Two pieces of pigskin were interlaced so that the area of the overlapping coverage area was set at about 1 cm². Then AHES and ACC solution were prepared in a Y-type double needle syringe system and the hydrogel precursor solution was injected into the overlapped area between the two pieces of pigskin. After that the overlapped area was loaded with a weight of 50 g for 1 h to allow the effective bonding of pigskins via AHES/ACC hydrogel. The bonding mechanical tensile properties were measured by using a Dejie DXLL-20000 materials testing instrument at a testing rate of 10 mm/min.

2.10. Cytotoxicity measurement of AHES/ACC hydrogel in vitro

The cytotoxicity of AHES/ACC hydrogel was evaluated by coculturing with bone marrow mesenchymal stem cells (BMSCs) in vitro for 1, 3 and 7 days. After anesthesia of SD rats, bone marrow was collected aseptically and cultured in a 5% CO₂ incubator at 37 °C. The complete medium was changed every 3 days to remove floating cells. The attached cells proliferated as primary BMSCs. When BMSCs reached 90% confluence after 7–10 days of primary culture, cells were digested and passaged at the ratio of 1:3. Then AHES/ACC hydrogels were prepared in the 24-well tissue culture plates and seeded with BMSCs at a density of 5×10^4 cells mL⁻¹. The complete medium was changed every day. At day 1, day 3, day 7 and day 14, the cell viability and proliferation of BMSCs were measured by CCK-8 assay. Firstly, the culture medium was replaced with 400 µl fresh complete medium containing 40 µl CCK-8 reaction solution to incubate for 4 h in a 5% CO₂ incubator at 37 °C. Then 100 µl of the complete medium was transferred to a 96-well tissue culture plate. The optical density value of absorbance at 450 nm was read using a multidetection microplate reader (MK3, Thermo, USA). The experiment was performed in triplicate and the results reflected the condition of BMSCs proliferation.

2.11. Blood coagulation test and biocompatibility measurement of AHES/ACC hydrogel in vivo

For in vivo blood coagulation test and biocompatibility measurement, AHES-4 and ACC-3 solution were prepared in a Y-type double needle syringe system. SD rat liver model was employed to evaluate the hemostasis properties of AHES/ACC hydrogel and medical gauze as a control. After 10% chloral hydrate (350 mg/kg) anesthesia of rats, the liver was exposed through abdominal midline incision. A small portion of liver was excised with scalpel and the wound was made at about 0.5×2 cm² in the right lobe of liver. The mixture precursor solution of hydrogel was injected onto the wound to promote blood coagulation and medical gauze was applied on the wound as a control. When the hemorrhage was visibly stopped and no bleeding was observed after removing medical gauze, the time from bleeding to stop was recorded as hemostasis time. 3×3 cm² filter papers were placed below the liver wound to absorb the blood. Blood loss amount was measured between control and hydrogel groups after weighing the medical gauze and filter paper with blood.

After that the hydrogel was preserved in the liver to further evaluate the biocompatibility in vivo. After 2 and 4 weeks, the rats were sacrificed and the liver samples were harvested. Tissues of heart, spleen, lung and kidney were also collected from rats. All specimens were fixed in neutral buffered paraformaldehyde and embedded in paraffin. The samples were sectioned at a thickness of 8.0 µm to stain with hematoxylin-eosin (H&E) and Masson's trichrome for histological observation. The animal experiment was conducted in accordance with the guidelines approved by the animal committee of Tongji University, China.

3. Results and discussion

3.1. Preparation of aldehyde hydroxyethyl starch (AHES)

3.1.1. Mechanism of oxidizing hydroxyethyl starch with sodium periodate

Fig. 1A showed the mechanism of using periodate to introduce dialdehydes. In this study, Hydroxyethyl starch was oxidized by sodium periodate to prepare aldehyde hydroxyethyl starch (AHES). Hydroxyethyl starch was (1 → 4)-linked β-D-glucoses with vicinal diols at C2 and C3. Given the specificity of periodate ions for vicinal diols, cleavage occurred between C2 and C3 [28]. Vicinal diols were oxidized to introduce dialdehydes. The amount of introduced dialdehyde group after periodate oxidation was dependent on the amount of sodium periodate. So, the oxidation reaction was carried out by using sodium periodate and hydroxyethyl starch in a molar ratio ($n(\text{NaIO}_4)/n(\text{HES})$) of 1, 1.5, 2 and 2.5, respectively. The obtained products were designated as AHES-1, AHES-2, AHES-3, AHES-4, respectively. Moreover, in the reaction process sodium periodate is easily decomposed by light. In order to avoid the formation of by-products during periodate oxidation, the reaction was carried out under light shielding conditions.

3.1.2. Structural characterization of aldehyde hydroxyethyl starch (AHES)

For confirming the introduction of dialdehyde group, FTIR spectrum was used. As shown in Fig. 1B, the broad absorption band appearing at 3500–3200 cm⁻¹ was associated with the intermolecular hydrogen bond O—H stretching vibration. The absorption band appearing at 2825 cm⁻¹ was characteristic for the aldehyde group C—H stretching vibration. The absorption band appearing at 1733 cm⁻¹ was characteristic for the aldehyde group C=O stretching vibration. Based on the absorption bands at 2825 cm⁻¹ and 1733 cm⁻¹, the presence of aldehyde group was confirmed in AHES molecule.

3.1.3. Determination of aldehyde group content

In order to illustrate the relationship between aldehyde group content and oxidant dosage, the aldehyde group content of AHES was determined by hydroxylamine hydrochloride titration method. The relationship between the aldehyde group content of AHES and the amount of oxidizing agent was shown in Fig. 1C below. It was revealed in Fig. 1C that the aldehyde group content of AHES was closely related to the amount of oxidizing agent NaIO₄. When the molar ratio of $n(\text{NaIO}_4)/n(\text{HES})$ was 1, the actual aldehyde group content was $52.45 \pm 2.27\%$, indicating that 52.45 ± 2.27% of glucopyranose rings in hydroxyethyl starch was oxidized by NaIO₄ to get aldehyde groups. As the relative amount of NaIO₄ increased ($n(\text{NaIO}_4)/n(\text{HES})$ from 1.5 to 2.5), the actual aldehyde group content of AHES increased from $63.90 \pm 2.36\%$ to $80.17 \pm 2.88\%$.

Theoretically, the mole of oxidized-opened glucopyranose ring is equivalent to the mole of sodium periodate. The aldehyde group content is equivalent to $n(\text{NaIO}_4)/n(\text{HES})$. However, the actual aldehyde group content value was less than the theoretical aldehyde group content value. The increment in the actual aldehyde group content value was also less than the increment in the theoretical aldehyde group content. As shown in Fig. 1D, the oxidation efficiency was getting lower and lower.

3.1.4. The relationship between aldehyde group content and reaction time

In order to explore the relationship between aldehyde group content and reaction time, aldehyde group content of AHES-3 was measured at different time point (1, 3, 5, 7, 10 h) during the oxidation reaction process. When the oxidation reaction was carried out for 1 h, 66.2% of glucopyranose rings in hydroxyethyl starch was oxidized and cleaved to get aldehyde groups, that is, aldehyde group content of AHES-3 was 66.2%. After that, aldehyde group content of AHES-3 was 74.3% at 3 h. And then aldehyde group content showed no significant change with the increase of the reaction time from 3 to 10 h. Thus, aldehyde group content of hydroxyethyl starch product had a significant increase and

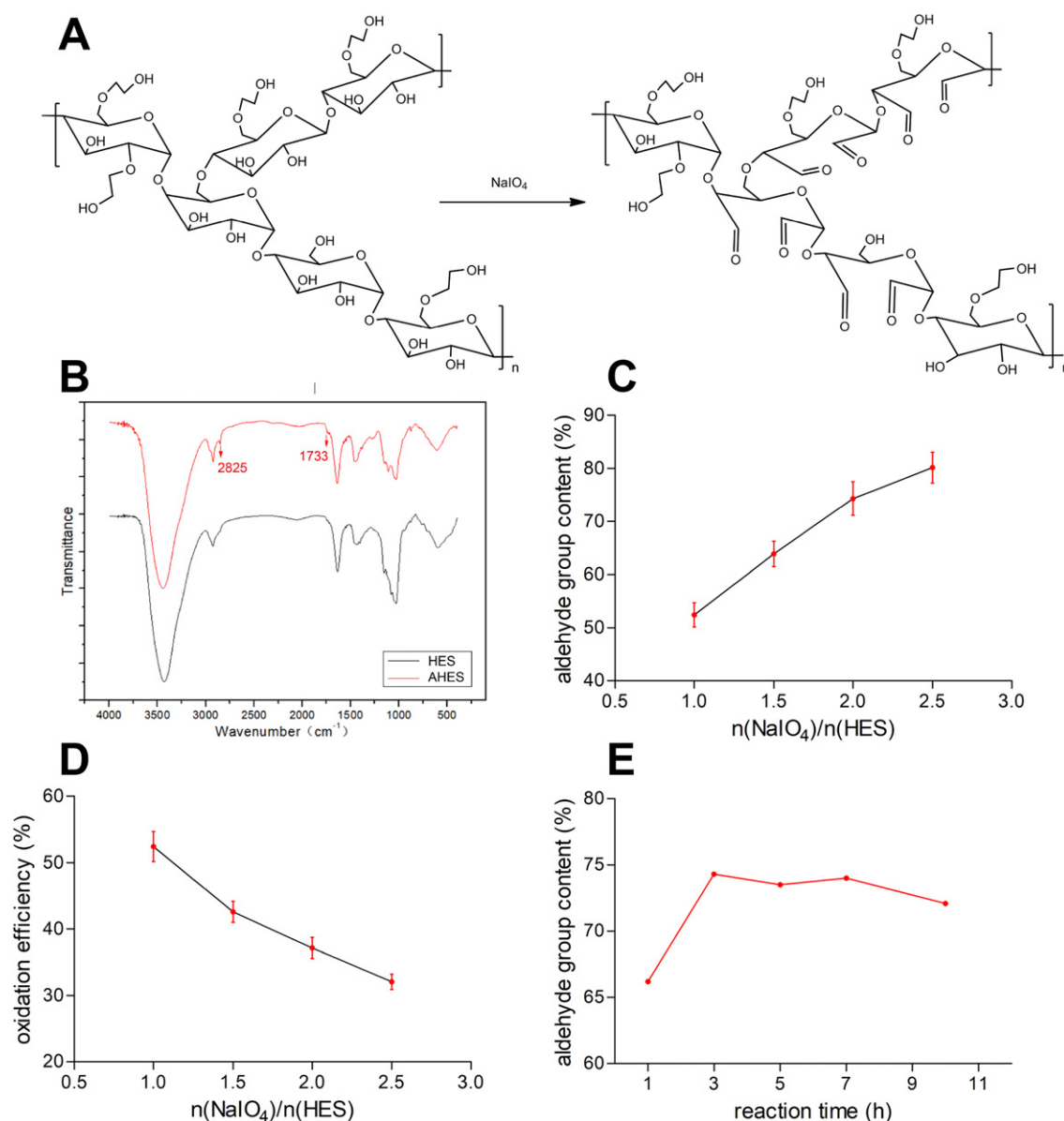


Fig. 1. A: Mechanism of periodate oxidation of hydroxyethyl starch; B: FTIR spectra of hydroxyethyl starch (HES) and aldehyde hydroxyethyl starch (AHES); C: the relationship between aldehyde group content and oxidant dosage; D: the relationship between oxidation efficiency and oxidant dosage; E: the relationship between aldehyde group content and reaction time.

reached a maximum within the first 3 h, and no longer increased with time (Fig. 1E).

3.2. Preparation of amino carboxymethyl chitosan

3.2.1. Modification of carboxymethyl chitosan using EDC and ethylenediamine

Carboxymethyl chitosan (CC) contains both carboxyl groups and amino groups, which is an ampholyte with amphoteric dissociation characteristics. Due to the intermolecular force between positively charged amino group and negatively charged carboxyl group, the solubility of CC in water is low at room temperature. Usually the saturated concentration of CC in aqueous solution is only 3% (w/v), which affects its full exploitation.

In the presence of EDC, the carboxyl group on the CC molecule was chemically modified by ethylenediamine to prepare amino carboxymethyl chitosan (ACC) with superior fluidity. The reaction was carried out in two steps (Fig. 2A). Firstly, the carboxyl group of CC reacted with EDC to form the intermediate product O-acylisourea. Then the intermediate O-acylisourea reacted with ethylenediamine to

form the amide of ACC, thereby grafting ethylenediamine onto the carboxymethyl chitosan to introduce more amino groups. The degree of the chemical conversion from carboxyl groups into amino groups depended on the amount of ethylenediamine. The chemical modification was performed by using ethylenediamine and carboxymethyl chitosan in a molar ratio ($n(\text{ED})/n(\text{COOH})$) of 5, 10, 20 and 30, respectively. The obtained products were designated as ACC-1, ACC-2, ACC-3, ACC-4, respectively.

3.2.2. Determination of amino group content

In the characteristic FTIR of amide stretching vibrations, the absorption band in the range of $1680\text{--}1600\text{ cm}^{-1}$ is usually connected with C=O bond of amide (Amide I band) while the absorption band in the range of $1550\text{--}1500\text{ cm}^{-1}$ is associated with N—H bond of amide (Amide II band). After chemical modification, ACC possessed moderately strong absorption bands near 1632 cm^{-1} and 1545 cm^{-1} . The 1632 cm^{-1} band was ascribed to the C=O stretching vibration ($\nu(\text{C=O})$) of ACC while the 1545 cm^{-1} band was ascribed to the N—H stretching vibration ($\nu(\text{N—H})$) of ACC (Fig. 2B). Thus, ethylenediamine

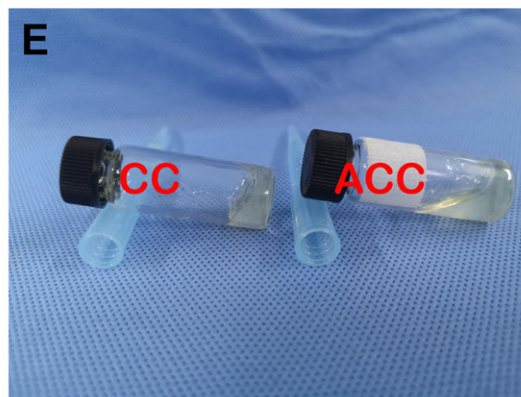
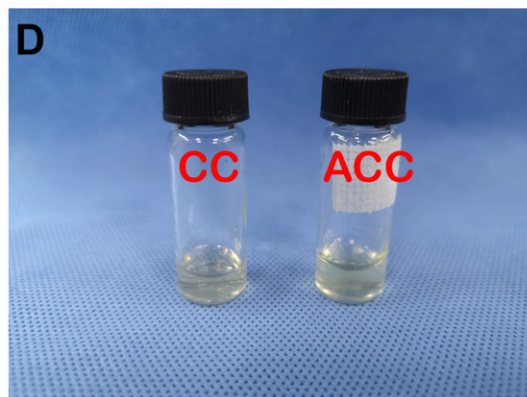
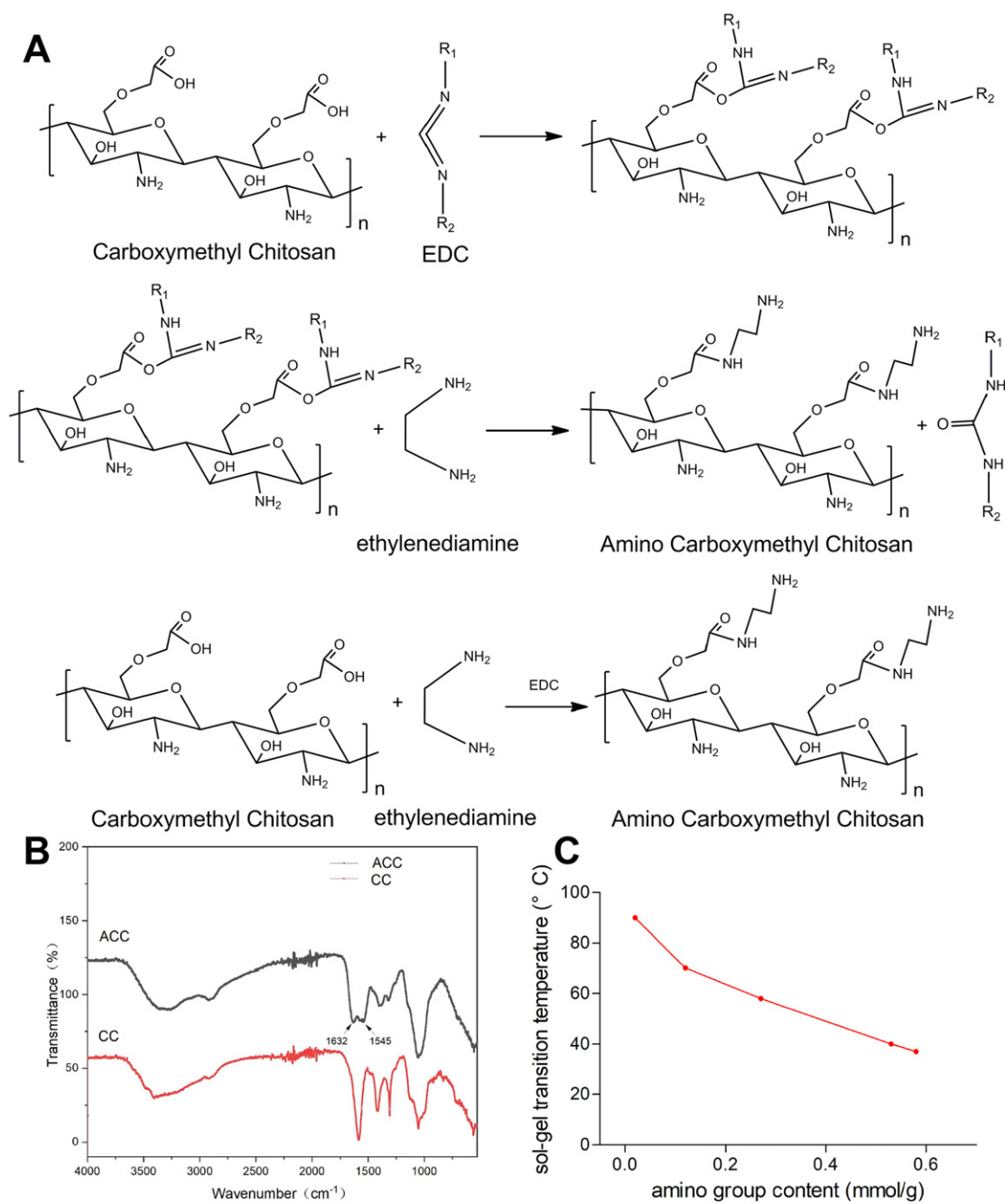


Fig. 2. A: Mechanism of modification of carboxymethyl chitosan using EDC and ethylenediamine; B: FTIR spectra of carboxymethyl chitosan (CC) and amino carboxymethyl chitosan (ACC); C: sol-gel transition temperature of ACC with various amino group content; D, E: illustration of the state of CC and ACC.

was successfully grafted onto the CC molecule to introduce more amino groups.

In the determination of amino group content, the amino of ACC reacted with sulfonic acid of TNBS to form an equimolar amount of trinitrophenylated (TNP) amino group and bisulfite ion. This method of measuring amino group content utilizes the phenomenon observed by Goldfarb, in which the sulfite can reversibly bind to the TNP amino group to form binding complexes with the maximum absorption near at 415 nm [29]. The amino content is related directly to the absorbance. Thus, a standard curve between the absorbance and the amino concentration was obtained firstly by measuring the absorbance of a gradient concentration of β -alanine reacted with TNBS. According to the formula for converting the amino group content and the absorbance value in the standard curve, the amine group content of ACC after chemical modification was calculated in Table 1.

First of all, the amino group content of CC was 0.02 mmol/g. That was, 1 g of CC contained 0.02 mmol amino group. After chemical modification ethylenediamine was grafted onto the CC molecule to introduce more amino groups. The amino group content of ACC was closely related to the amount of ethylenediamine. When the molar ratio of $n(\text{ED})/n(\text{COOH})$ was 5, the amino group content was 0.12 mmol/g and carboxyl modification efficiency was 12%. With the increase of $n(\text{ED})/n(\text{COOH})$ from 5 to 30, the amino group content and carboxyl modification efficiency increased significantly from 0.12 to 0.58 and from 12% to 70% respectively.

3.2.3. Fluidity assessment of ACC after chemical modification

At room temperature carboxymethyl chitosan solution had lower fluidity and exhibited a gel state while incubating in a hot water bath carboxymethyl chitosan solution appeared to flow. The sol-gel transition temperature indicated that there was attraction force between positively charged amino group and negatively charged carboxyl group in carboxymethyl chitosan solution. The lower sol-gel transition temperature, the weaker attraction force. By grafting ethylenediamine on carboxymethyl chitosan, carboxyl groups were converted to amino groups, which weakened the attraction between positively charged amino group and negatively charged carboxyl group. As shown in Fig. 2C, ACC had a lower sol-gel transition temperature than the unmodified CC. With the increase of amino group content, the sol-gel transition temperature gradually decreased. This was due to the weakened attraction between positively charged amino group and negatively charged carboxyl group after carboxyl groups converting to amino groups. As a result, ACC in water had better fluidity at room temperature and obtained higher solubility. Compared with CC, ACC in aqueous solution possessed better fluidity at room temperature (Fig. 2D, E), consequently facilitating the injection of ACC solution to some extent. Moreover, as the amino group content in the molecular chain increased, the distribution of positively charged amino groups in the aqueous solution increased. Under the repulsion of positive charges, the molecular chain stretched, thereby improving the water solubility. In this study, after chemical modification the maximum concentration at room temperature increased from 3% w/v to 10% w/v.

3.3. Gel formation and gelation time of AHES/ACC hydrogel

3.3.1. Mechanism of gel formation for AHES/ACC hydrogel

The Schiff base reaction was proposed by the German chemist Hugo Schiff in 1864 [30,31]. It refers to the reaction between aldehyde (or ketone) groups and amino groups to produce imine groups ($-\text{C}=\text{N}-$). In this study hydroxyethyl starch was oxidized by sodium periodate to get aldehyde groups and carboxymethyl chitosan was modified to get more amino groups. The chemical modification of the two-component precursor was to provide more reactive groups, thereby increasing the contact frequency of reactive groups between the molecules. After mixing AHES and ACC solutions, more crosslinking sites with imine bonds ($-\text{C}=\text{N}-$) were connected, resulting in an injectable hydrogel

Table 1
Measurement of amino group content.

Sample	$n(\text{ED})/n(\text{COOH})$	$-\text{NH}_2$ amino group content (mmol/g)	$-\text{COOH}$ carboxyl modification efficiency (%)
CC	0	0.02	0
ACC-1	5	0.12	12
ACC-2	10	0.27	31
ACC-3	20	0.53	63
ACC-4	30	0.58	70

with special characteristics (Fig. 3A). As showed in Fig. 3B, gel formation occurred quickly after mixing AHES and ACC solutions.

3.3.2. Structural characterization of AHES/ACC hydrogel

Fig. 3C showed the FTIR spectrum of AHES/ACC hydrogel, AHES and ACC. The absorption band appearing at 1730 cm^{-1} in AHES was characteristic for the aldehyde group $\text{C}=\text{O}$ stretching vibration. The absorption band appearing at 1632 cm^{-1} in ACC was associated with the amide group $\text{C}=\text{O}$ stretching vibration, indicating ethylenediamine was grafted on CC. After mixing AHES and ACC, Schiff base reaction was carried out. The absorption band at 1730 cm^{-1} and 1632 cm^{-1} disappeared and a new stretching vibration peak appeared at 1670 cm^{-1} in the infrared spectrum of the AHES/ACC hydrogel. Generally, the stretching vibration peak of imine bond ($\text{C}=\text{N}$) was between 1650 cm^{-1} and 1700 cm^{-1} . Therefore, imine bonds were formed in AHES/ACC hydrogel, proving the Schiff base reaction mechanism described above.

3.3.3. Gelation time measurement of AHES/ACC hydrogel

Gelation time was used to evaluate the time of two-component hydrogel formation when AHES and ACC solutions were mixed together. It was an important parameter to measure the speed of gel formation. If gelation time is too long, the hydrogel precursor solutions are easily lost in the body and not conducive to gel formation. If gelation time is too short, the hydrogel is formed too fast. It is unfavorable to mix other pharmaceutical reagents for therapy, resulting in loss of injectability. Thus, suitable gelation time is essential for hydrogel to achieve simple formulation and convenient administration under physiological conditions.

In this experiment, the magnetic bead rotation method was used to determine the gelation time and the stopwatch was used to record the time from mixing of two components to loss of fluidity. The gelation time of six formulated hydrogels were shown in Fig. 3D. AHES of different aldehyde group content was crosslinked with ACC of different amino group content quickly. All the gelation time was shorter than 20 s. During the formation process of AHES/ACC two-component hydrogel, gelation time was significantly affected by the content of aldehyde and amino group. As showed in Fig. 3E, AHES solution with different aldehyde group content was mixed with ACC-2 solution with 0.27 mmol/g $-\text{NH}_2$ group. With the increase of aldehyde group content, gelation time decreased significantly. Owing to greater oxidation degree of HES, more $-\text{CHO}$ groups were introduced into the molecular chain of AHES. When the Schiff base reaction occurred, more reactive sites made the crosslinking reaction more efficient. The time to reach the gel point was shorter. Similarly, when more $-\text{NH}_2$ groups were introduced into ACC, the crosslinking efficiency of $-\text{NH}_2$ with $-\text{CHO}$ increased. In the gel formation of different $-\text{NH}_2$ content ACC mixed with AHES-4, shorter gelation time was achieved by increasing amino content (Fig. 3F). Thus, whether introducing more aldehyde groups or grafting more amino groups the frequency of intermolecular Schiff base reaction can be increased to reach a shorter gelation time.

3.4. Equilibrium swelling analyses of AHES/ACC hydrogel

Fig. 4 showed the equilibrium water content and swelling ratio of AHES/ACC hydrogels. The equilibrium water content of all AHES/ACC

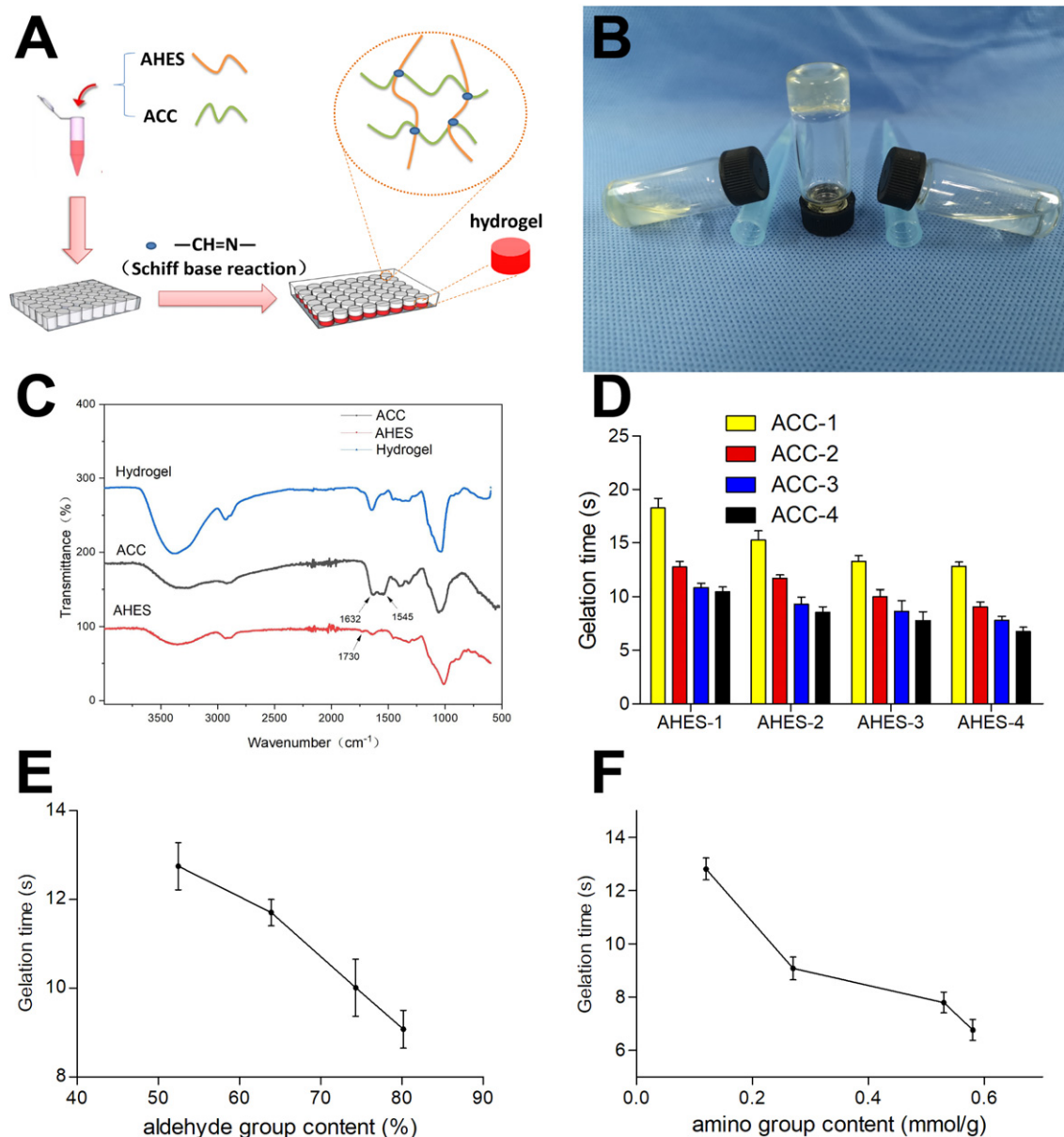


Fig. 3. A: Mechanism of gel formation for AHES/ACC hydrogel; B: gelation occurred quickly after mixing the two components; C: FTIR spectra of AHES/ACC hydrogel, AHES and ACC; D: gelation time of AHES/ACC hydrogels with various contents of aldehyde and amino group; E: the relationship between gelation time and aldehyde group content; F: the relationship between gelation time and amino group content.

hydrogels was above 90%, indicating that large amounts of water were retained in hydrogel polymeric networks (Fig. 4A). Due to this property, AHES/ACC hydrogels are more like natural soft tissues than any other type of biomaterials. Compared with AHES-2/ACC-2 hydrogel, AHES-2/ACC-3 hydrogel exhibited a lower equilibrium swelling ratio. AHES-2/ACC-3 hydrogel possessed higher amino group content, resulting in higher crosslinking density. So that the swelling ratio of AHES-2/ACC-3 hydrogel was lower than AHES-2/ACC-2 hydrogel. The same results were also observed between AHES-3/ACC-2 and AHES-3/ACC-3 hydrogel, AHES-4/ACC-2 and AHES-4/ACC-3 hydrogel (Fig. 4B).

Except for the content of amino group, the amount and density of crosslinking sites was also dependent on the aldehyde group content. As for ACC-2 with the increase in content of the aldehyde groups from AHES-2 to AHES-4, the two-component hydrogels exhibited a decreased equilibrium swelling ratio (Fig. 4C). The swelling ratio of AHES-4/ACC-2 hydrogel was lower than AHES-3/ACC-2 and AHES-2/ACC-2 hydrogel. This was ascribed to the higher aldehyde group content of AHES-4 than AHES-3 and AHES-2. The increased content of aldehyde

groups in two-component hydrogel system generated more crosslinking sites to suppress the capacity for water absorption. Similarly, the same decreased tendency was observed as for ACC-3 with AHES-2 to AHES-4 (Fig. 4D).

Thus, the content of aldehyde and amino group plays an important role in the equilibrium swelling properties of AHES/ACC hydrogels. Whether increasing aldehyde group content of AHES or increasing amino group content of ACC, more imine bonds will be formed in the Schiff base reaction. Consequently, the crosslinking and binding sites increase in this two-component hydrogel so that the hydrogel network will be denser. As a result, equilibrium water content and swelling ratio will be lower.

3.5. In vitro degradation analyses of AHES/ACC hydrogel

Fig. 5 showed the in vitro degradation of different formulated AHES/ACC hydrogels and revealed the effect of aldehyde or amino group content on the weight loss of hydrogels. During the entire experimental

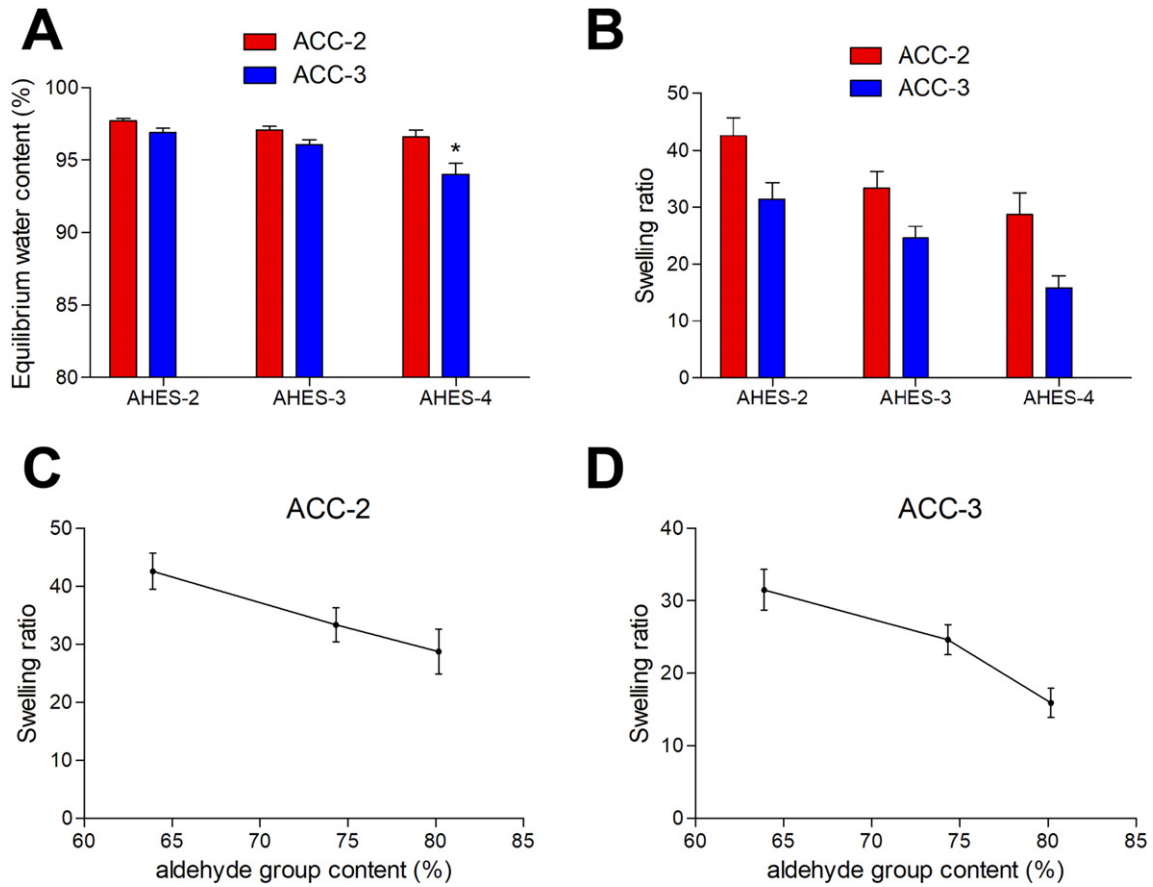


Fig. 4. A: Equilibrium water content of AHES/ACC hydrogels with various contents of aldehyde and amino group at the equilibrium swelling state; B: swelling ratio of AHES/ACC hydrogels at the equilibrium swelling state; C: the relationship between swelling ratio and aldehyde group content for ACC-2; D: the relationship between swelling ratio and aldehyde group content for ACC-3.

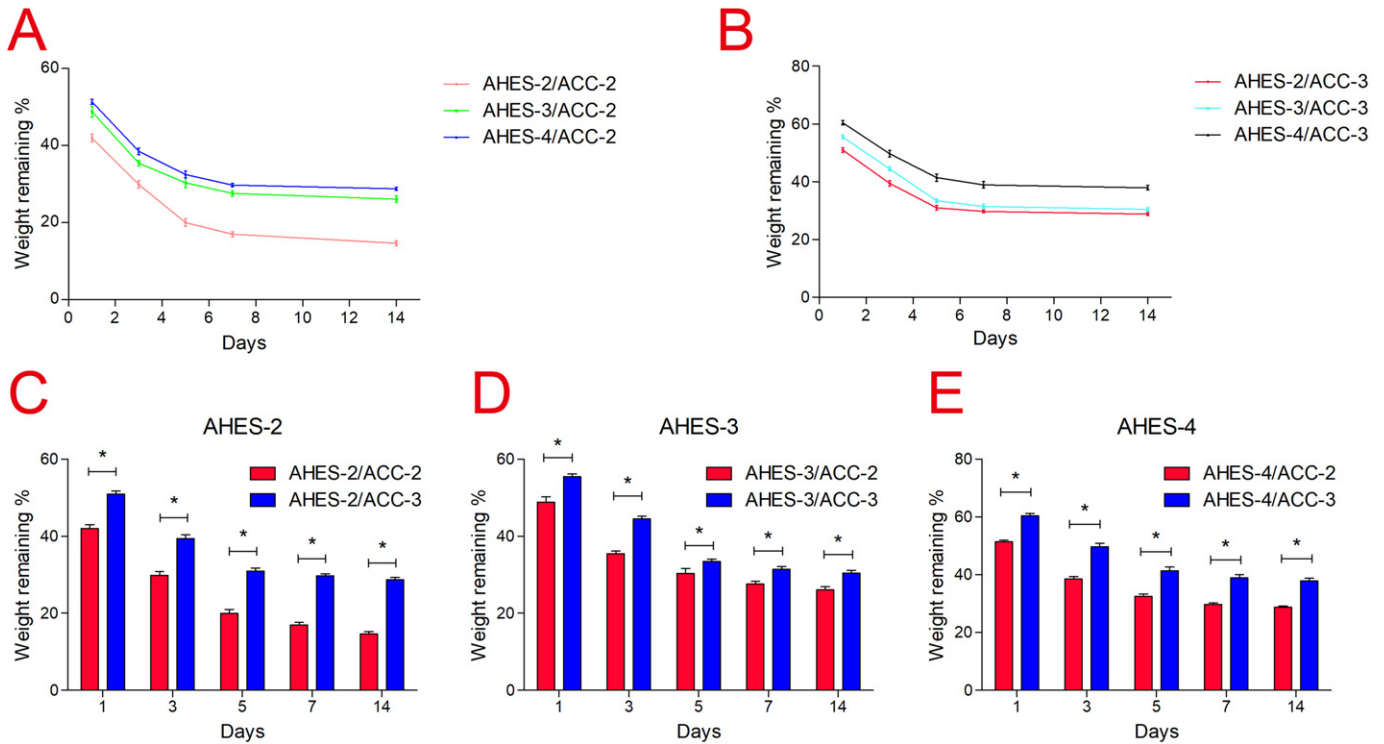


Fig. 5. In vitro degradation properties of AHES/ACC hydrogel. A: Degradation property of ACC-2 hydrogel with different aldehyde group content at different time points. B: A: Degradation property of ACC-3 hydrogel with different aldehyde group content at different time points. C, D, E: The effect of amino group on degradation property of AHES-2, AHES-3 and AHES-4 hydrogels.

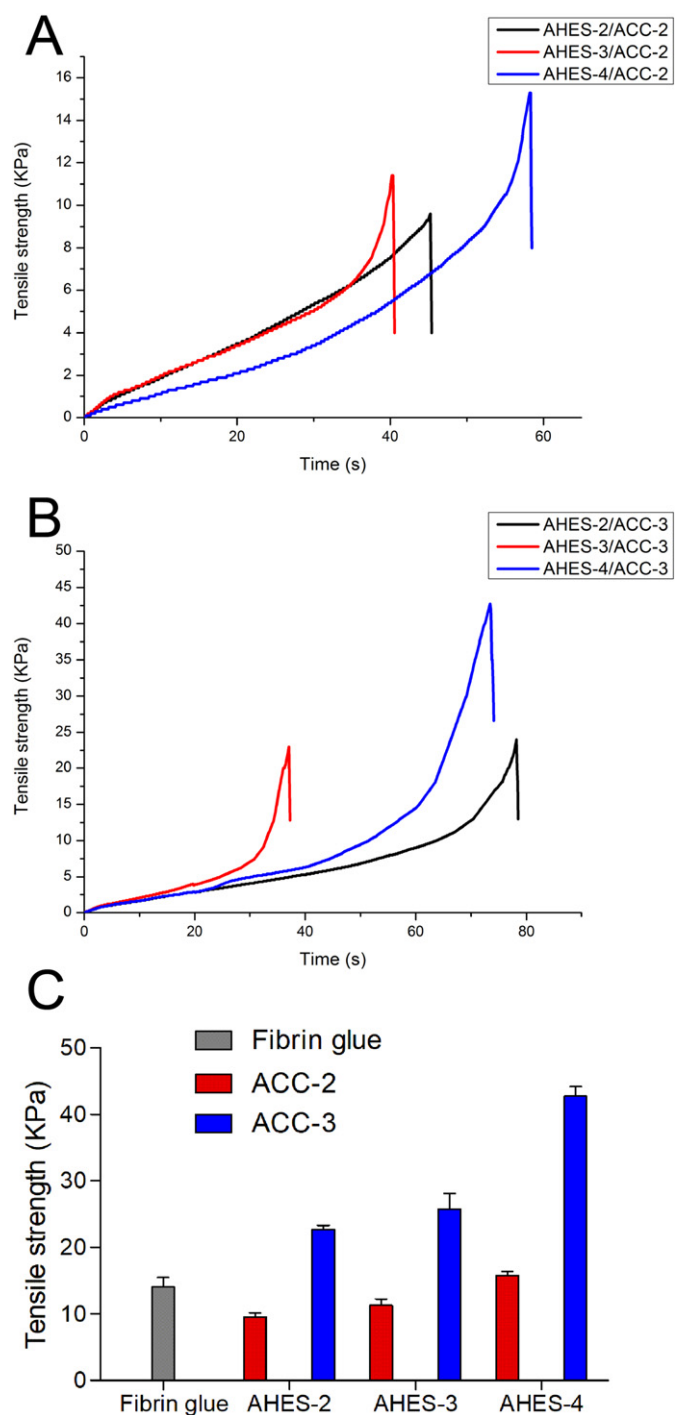


Fig. 6. Mechanical tensile test of AHES/ACC hydrogel. A: Mechanical tensile strength of ACC-2 hydrogel with different aldehyde group content; B: Mechanical tensile strength of ACC-3 hydrogel with different aldehyde group content; C: The effect of amino group on mechanical tensile strength of AHES-2, AHES-3 and AHES-4 hydrogels and mechanical comparison with commercial fibrin glue sealant.

period, all formulated AHES/ACC hydrogels degraded over time (Fig. 5A & B). There were two distinct phases of degradation process. During the first 5 days, all formulated AHES/ACC hydrogels had a significant weight loss. This was ascribed to hydrolysis of hydrogels, a rapid degradation process at physiologically relevant conditions. This phase included overwhelming physical process of dissolution and infrequent chemical process of three-dimensional polymer network structure cleavage. In the following days from day 5 to day 10, the weight loss of AHES/ACC hydrogels became slight. This was ascribed to chemical degradation of

AHES/ACC hydrogel backbone. Thus, the AHES/ACC hydrogels could degrade *in vitro* through two mechanisms: hydrolysis as fast and chemical degradation of molecular backbone as steady.

In the meantime, aldehyde and amino group content exerted an important influence on the degradation properties of hydrogels. As shown in Fig. 5A, with the increase in content of the aldehyde groups from AHES-2 to AHES-4, the two-component hydrogels exhibited a decreased degradation rate. The weight remaining of AHES-4/ACC-2 hydrogel was significantly higher than AHES-3/ACC-2 and AHES-2/ACC-2 hydrogel. The same results were observed in AHES-4/ACC-3, AHES-3/ACC-3 and AHES-2/ACC-3 hydrogels (Fig. 5B). Furthermore, with the increase in content of the amino groups from ACC-2 to ACC-3, a decreased degradation rate was also observed. Compared with AHES-2/ACC-2 hydrogel, AHES-2/ACC-3 hydrogel possessed higher weight remaining after 14 days of degradation (Fig. 5C). The same results were observed by comparing AHES-3/ACC-2 and AHES-3/ACC-3 hydrogel (Fig. 5D), AHES-4/ACC-2 and AHES-4/ACC-3 hydrogel (Fig. 5E).

This phenomenon was ascribed to the relation between crosslinking density and degradation rate. The degradation behavior of hydrogels is generally considered to depend on the crosslink density. High crosslink density can retard the degradation of hydrogels [32]. With the increase in content of amino or aldehyde group, the two-component hydrogels possessed more crosslinking sites, resulting in a decreased degradation rate.

3.6. Mechanical tensile test of AHES/ACC hydrogel

For future application as soft tissue adhesive, mechanical tensile force is an important parameter. The mechanical tensile test of different formulated AHES/ACC hydrogels was performed by measuring pigskin adhesive strength to illustrate the effect of aldehyde or amino group content on tensile strength of hydrogels. As shown in Fig. 6A, with the increase of aldehyde group content in AHES from AHES-2 to AHES-4, the tensile strength of the formed hydrogel for ACC-2 gradually increased. When the aldehyde group of AHES reached the highest content of 80% in AHES-4, the hydrogel had the highest tensile strength of 15.83 ± 0.41 kPa. The same results were observed as for ACC-3 with the increase of aldehyde group content from AHES-2 to AHES-4 (Fig. 6B). Except for aldehyde group content, the content of amino group also exerted an effect on the tensile strength of hydrogels. Compared with ACC-2 hydrogel, ACC-3 hydrogel exhibited an increased strength due to higher amino group content. Thus, AHES-4/ACC-3 hydrogel with the higher aldehyde and amino group content than others, reached the highest tensile strength of 42.73 ± 1.18 kPa (Fig. 6C).

3.7. Cytotoxicity measurement of AHES/ACC hydrogel *in vitro*

Cytotoxicity measurement of AHES/ACC hydrogel *in vitro* was performed by seeding BMSCs onto hydrogel surfaces. During the entire culture period, BMSCs onto different formulated AHES/ACC hydrogel surfaces displayed a significant increased viability profile (Fig. 7A & B). The number of viable BMSCs onto all hydrogel surfaces increased with culturing time. This revealed that AHES/ACC hydrogel displayed a good biocompatibility *in vitro* and not hampered proliferation of BMSCs on matrix surface.

Further observation and analysis, there were conspicuous difference in cell viability and proliferation between AHES/ACC hydrogels with different aldehyde or amino group content. As for ACC-2 with the increase in content of the aldehyde groups from AHES-1 to AHES-4, the two-component hydrogels exhibited an increased cytotoxicity property, which is unfavorable for cell viability and proliferation (Fig. 7C). BMSCs cultured on AHES-4/ACC-2 hydrogel had a lower proliferative capacity than AHES-3/ACC-2, AHES-2/ACC-2 and AHES-1/ACC-2 hydrogel. This was ascribed to the highest aldehyde group content of AHES-4 in these four groups. The presence of aldehyde groups in large content was not conducive to cell viability and proliferation. Similarly, the

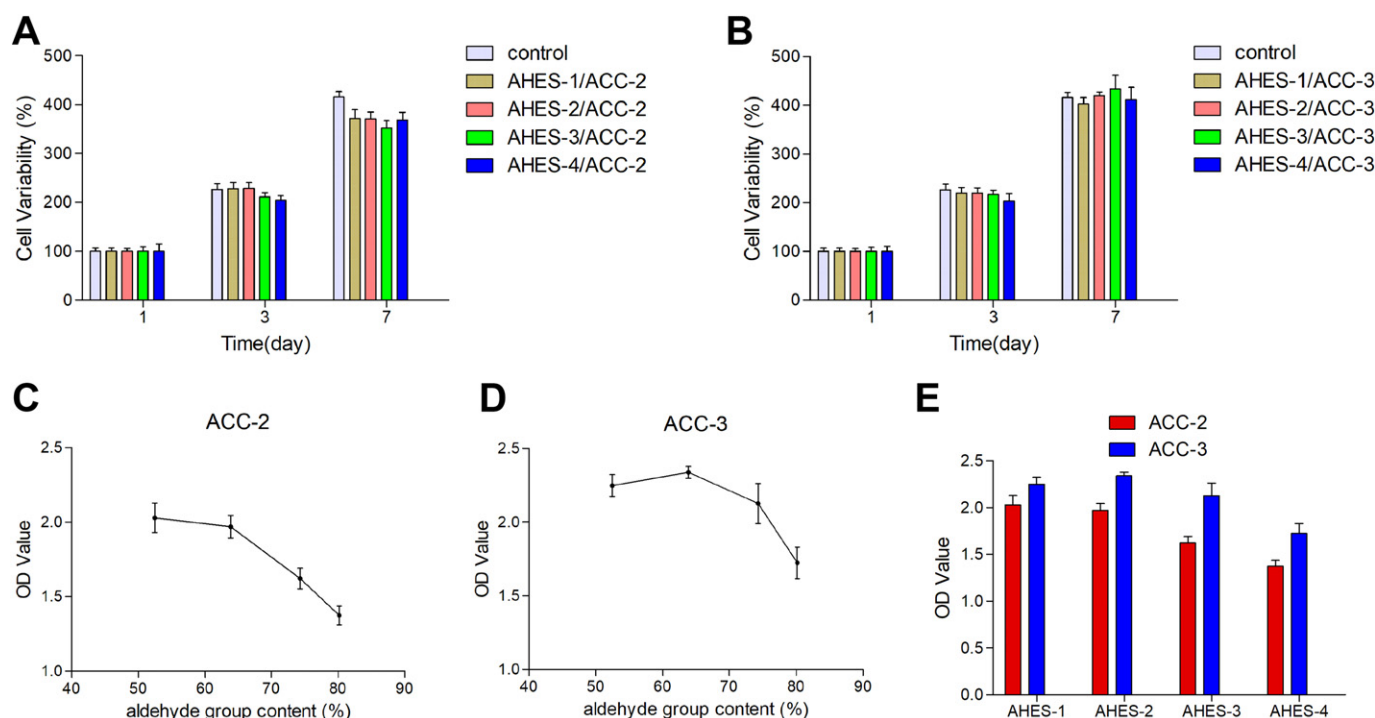


Fig. 7. Cytotoxicity measurement of AHES/ACC hydrogel in vitro. BMSCs were cultured onto different formulated AHES/ACC hydrogel surfaces for 1, 3 and 7 days (A, B). C: Cell compatibility of ACC-2 hydrogel with different aldehyde group content; D: cell compatibility of ACC-3 hydrogel with different aldehyde group content; E: the effect of amino group on cell compatibility of AHES-1, AHES-2, AHES-3 and AHES-4 hydrogels.

same results were observed as for ACC-3 with AHES-1 to AHES-4 (Fig. 7D). AHES-4/ACC-3 hydrogel, possessing higher aldehyde group content than others, correspondingly exhibited an increased cytotoxicity property than AHES-3/ACC-3, AHES-2/ACC-3 and AHES-1/ACC-3 hydrogel.

Interestingly, unlike the effect of aldehyde group, the effect of amino group on cell viability and proliferation is completely manifested as another result. Compared with AHES-4/ACC-2 hydrogel, AHES-4/ACC-3 hydrogel possessing higher amino group content, exhibited a favorable effect on cell viability and proliferation. The same results were also observed in AHES-3/ACC-2 versus AHES-3/ACC-3, AHES-2/ACC-2 versus AHES-2/ACC-3 and AHES-1/ACC-2 versus AHES-1/ACC-3 (Fig. 7E). The OD value in ACC-3 groups was higher than that in ACC-2 groups, indicating that the presence of amino groups was conducive to cell viability and proliferation. One possible explanation is that the positively charged $-NH_2$ group facilitates cell membrane adhesion with negative sites and provides a better environment for cell growth, thus exhibiting better cell compatibility.

3.8. Blood coagulation test and biocompatibility measurement of AHES/ACC hydrogel in vivo

The hemostasis efficacy of AHES/ACC hydrogel in vivo was assessed by a SD rat liver model shown in Fig. 8A. For comparison, AHES-4 and ACC-3 solution were employed to prepare AHES/ACC hydrogel and medical gauze commonly used in clinics was designated as a control. When the wound was made in the liver, the bleeding was not effectively stopped shown in Fig. 8B. After the AHES/ACC hydrogel was injected onto the cut wound, the blood coagulation was carried out shown in Fig. 8C. The hemostasis time of AHES/ACC hydrogel was observed to be 31.8 ± 5.42 s, which was significantly shorter than that of control group (Fig. 8D). The blood loss amount of AHES/ACC hydrogel was also significantly less than that of control group (Fig. 8E). The mechanism of hemostasis for AHES/ACC hydrogel may be the combination of physical occlusive compression and biological activation. At the site of the wound, injectable AHES/ACC hydrogel gels in situ, forming a

three-dimensional network structure as a physical blockage of the wound. This can effectively prevent bleeding and blood loss. Then, AHES/ACC hydrogel exposes amino groups to the blood. Due to the specific binding of negatively charged platelets with positively charged amino groups, blood coagulation process is biological activated to accelerate hemostasis [33]. Thus, AHES/ACC hydrogel has effective hemostatic ability and may be potential for use as tissue adhesives and hemostatic wound dressings in clinic.

After blood coagulation test the hydrogel was preserved in the liver to further evaluate the biocompatibility in vivo. The goal of in vivo measurement of AHES/ACC hydrogel was to determine the biocompatibility and safety of this hydrogel in a biological environment. At 2 and 4 weeks after treatment, all rats were alive and no harmful effects were observed. In the histological examination of liver wound treated with AHES/ACC hydrogel, there was no inflammatory response through activation of white blood cells and cell death or injury (Fig. 8F). Moreover, systemic toxicity was estimated through investigating the potential harmful effects on vital organs of heart, spleen, lung and kidney (Fig. 8G). Masson's trichrome staining was also performed to identify fibrosis and macrophage infiltration (Fig. 9). There were no fibrosis and macrophage infiltration detectable in the liver and other vital organs. All the histological staining results showed that these tissues exhibited normal architectural arrangements, indicating that AHES/ACC hydrogel and its metabolites or released components have no systemic toxic effect on the host vital organs.

4. Conclusion

In situ forming hydrogel composed of aldehyde hydroxyethyl starch and amino carboxymethyl chitosan can be modulated as a promising scaffold to satisfy specific needs for biomedical applications. Various contents of aldehyde and amino group were achieved by changing the molar ratio of sodium periodate to hydroxyethyl starch ($n(\text{NaIO}_4)/n(\text{H})$) and ethylenediamine to carboxymethyl chitosan ($n(\text{ED})/n(\text{COOH})$). Two-component AHES/ACC hydrogels with various contents of aldehyde and amino group were formed through Schiff base reaction.

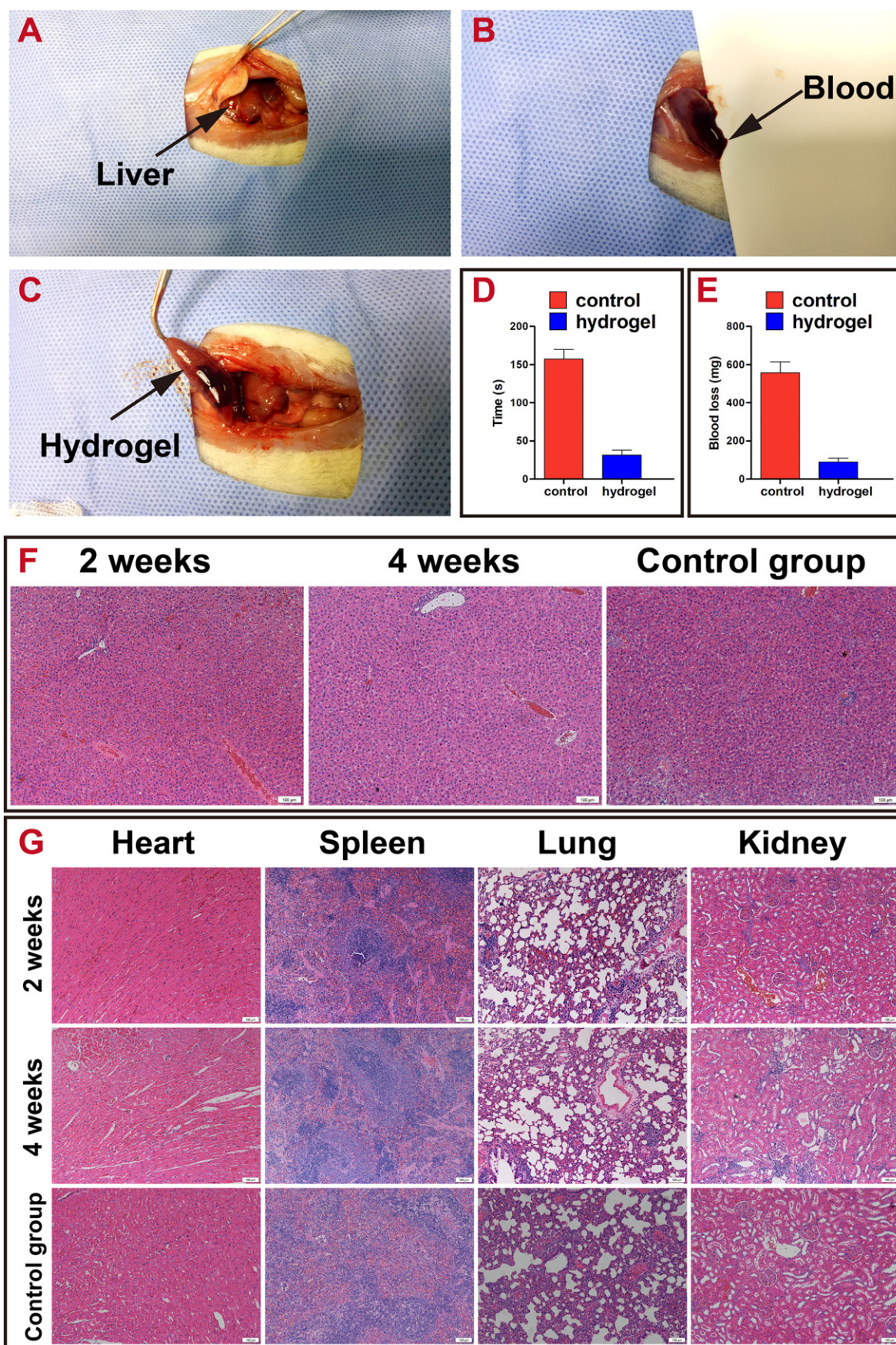


Fig. 8. Blood coagulation test and biocompatibility measurement of AHES/ACC hydrogel in vivo. The hemostasis efficacy of AHES/ACC hydrogel was assessed by a SD rat liver model (A, B, C). Hemostasis time (D) and blood loss amount (E) were statistically analyzed. Liver (F) and other organs (G) were observed and compared with normal tissue (control group) to evaluate biocompatibility of AHES/ACC hydrogel in vivo at different time points (2 and 4 weeks). Scale bar represents 100 μ m.

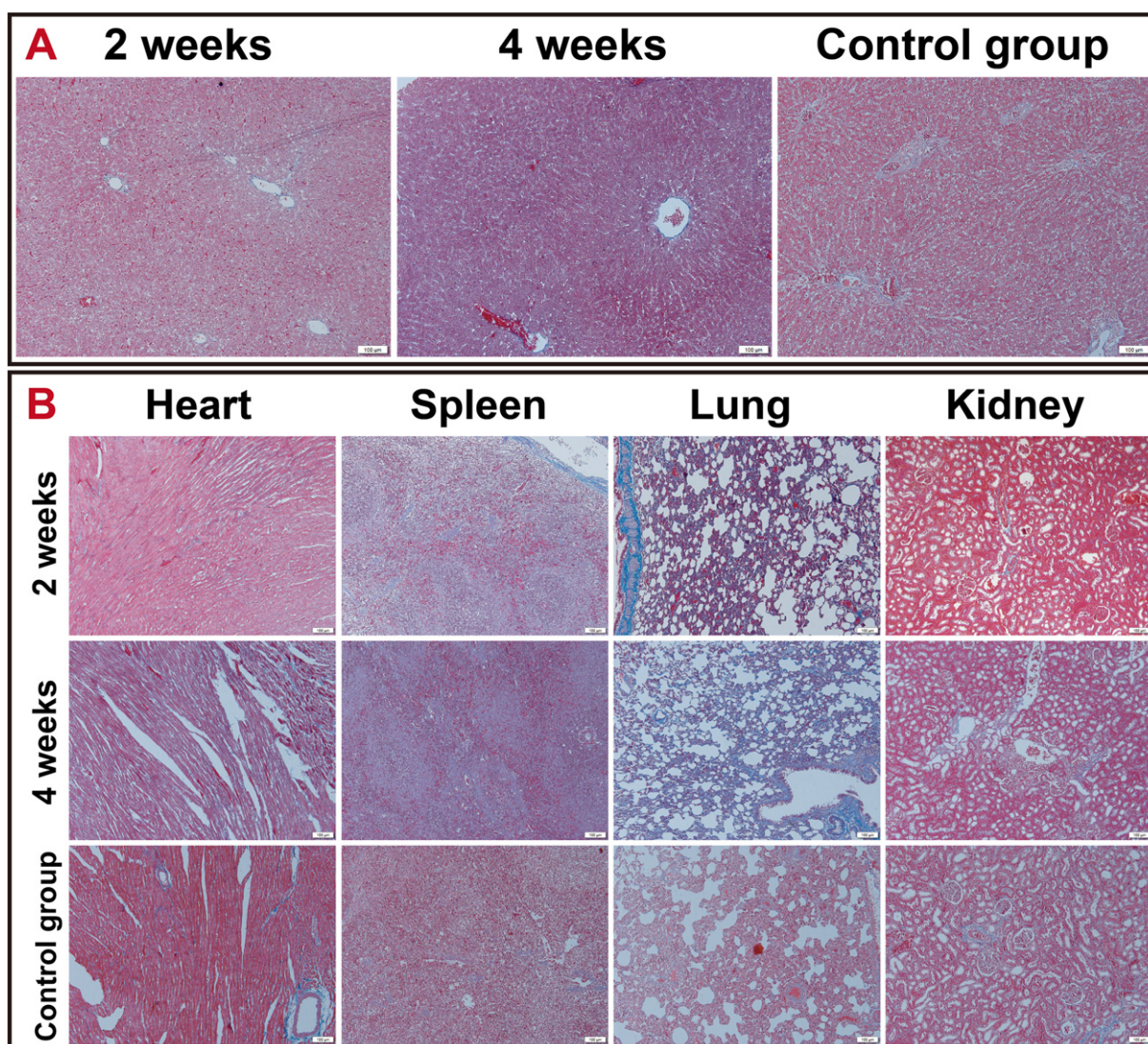


Fig. 9. Liver (A) and other organs (B) were observed and compared with normal tissue (control group) through Masson's trichrome staining to evaluate biocompatibility of AHES/ACC hydrogel in vivo at different time points (2 and 4 weeks). Scale bar represents 100 μm .

The physical properties of AHES/ACC hydrogels could be modulated including gelation time, swelling ratio, degradation and mechanical tensile. When the content of amino and aldehyde group increased, the two-component hydrogels possessed more crosslinking sites and higher crosslinking density, resulting in shorter gelation time, lower swelling ratio, lower degradation rate and higher mechanical tensile strength. Moreover, cell cytotoxicity of AHES/ACC hydrogels in vitro showed that AHES/ACC hydrogels supported cell viability and proliferation of BMSCs. Biocompatibility measurement in vivo showed that AHES/ACC hydrogels were non-toxic to vital organs of heart, liver, spleen, kidney and kidney, exhibiting good biodegradability and biocompatibility in vivo. Blood coagulation test indicated that AHES/ACC hydrogel possessed effective soft tissue adhesive and wound hemostasis capacity. Therefore, according to this study, the injectable AHES/ACC hydrogel can be manipulated and applied in wound hemostasis, soft tissue adhesive and other biomedical applications in future.

CRediT authorship contribution statement

Jia Liu: Conceptualization, Methodology, Visualization, Investigation, Writing - original draft. **Jun Li:** Investigation, Visualization, Writing - original draft. **Fan Yu:** Validation, Formal analysis, Visualization. **Yaxin Zhao:** Investigation, Data curation. **Xiu-mei Mo:** Data curation,

Supervision, Writing - review & editing. **Jian-feng Pan:** Supervision, Data curation, Writing - review & editing.

Acknowledgements

This work was financially supported by the National Natural Science Foundation of China (Contract Grant No. 81802144) and the Fundamental Research Funds for the Central Universities (Contract Grant No. 22120180582) and the Research Project of Shanghai Municipal Population and Family Planning Commission (Contract Grant No. 20164Y0050).

Appendix A. Supplementary data

Supplementary data to this article can be found online at <https://doi.org/10.1016/j.ijbiomac.2020.01.005>.

References

- [1] J.M. Zhu, R.E. Marchant, Design properties of hydrogel tissue-engineering scaffolds, *Expert Rev. Med. Devices* 8 (2011) 607–626.
- [2] J. Lee, M.J. Cuddihy, N.A. Kotov, Three-dimensional cell culture matrices: state of the art, *Tissue Eng. Part B Rev.* 14 (2008) 61–86.

- [3] H. Geckil, F. Xu, X.H. Zhang, S. Moon, U. Demirci, Engineering hydrogels as extracellular matrix mimics, *Nanomedicine* 5 (2010) 469–484.
- [4] N.C. Hunt, L.M. Grover, Cell encapsulation using biopolymer gels for regenerative medicine, *Biotechnol. Lett.* 32 (2010) 733–742.
- [5] S.Q. Liu, R. Tay, M. Khan, P.L.R. Ee, J.L. Hedrick, Y.Y. Yang, Synthetic hydrogels for controlled stem cell differentiation, *Soft Matter* 6 (2010) 67–81.
- [6] G.D. Nicodemus, S.J. Bryant, Cell encapsulation in biodegradable hydrogels for tissue engineering applications, *Tissue Eng. Part B Rev.* 14 (2008) 149–165.
- [7] S. Seiffert, J. Sprakel, Physical chemistry of supramolecular polymer networks, *Chem. Soc. Rev.* 41 (2012) 909–930.
- [8] W.E. Hennink, C.F. van Nostrum, Novel crosslinking methods to design hydrogels, *Adv. Drug Deliv. Rev.* 64 (2012) 223–236.
- [9] Z.W. Zeng, X.M. Mo, C.L. He, Y. Morsi, H. El-Hamshary, M. El-Newehy, An in situ forming tissue adhesive based on poly(ethylene glycol)-dimethacrylate and thiolated chitosan through the Michael reaction, *J. Mater. Chem. B* 4 (2016) 5585–5592.
- [10] Z.W. Zeng, X.M. Mo, Rapid in situ cross-linking of hydrogel adhesives based on thiol-grafted bio-inspired catechol-conjugated chitosan, *J. Biomater. Appl.* 32 (2017) 612–621.
- [11] B. Bi, M.S. Ma, S.Y. Lv, R.X. Zhuo, X.L. Jiang, In-situ forming thermosensitive hydroxypropyl chitin-based hydrogel crosslinked by Diels-Alder reaction for three dimensional cell culture, *Carbohydr. Polym.* 212 (2019) 368–377.
- [12] M. Barati, S.M. Samani, L.P. Jahromi, H. Ashrafi, A. Azadi, Controlled-release in-situ gel forming formulation of tramadol containing chitosan-based pro-nanogels, *Int. J. Biol. Macromol.* 118 (2018) 1449–1454.
- [13] J.J. Huang, Y.M. Deng, J.A. Ren, G.P. Chen, G.F. Wang, F. Wang, et al., Novel in situ forming hydrogel based on xanthan and chitosan re-gelifying in liquids for local drug delivery, *Carbohydr. Polym.* 186 (2018) 54–63.
- [14] K.Y. Lu, Y.C. Lin, H.T. Lu, Y.C. Ho, S.C. Weng, M.L. Tsai, et al., A novel injectable in situ forming gel based on carboxymethyl hexanoyl chitosan/hyaluronic acid polymer blending for sustained release of berberine, *Carbohydr. Polym.* 206 (2019) 664–673.
- [15] Y.L. Li, Y. Tan, K. Xu, C.G. Lu, X.C. Liang, P.X. Wang, In situ crosslinkable hydrogels formed from modified starch and O-carboxymethyl chitosan, *RSC Adv.* 5 (2015) 30303–30309.
- [16] E.A. Kamoun, N-succinyl chitosan-dialdehyde starch hybrid hydrogels for biomedical applications, *J. Adv. Res.* 7 (2016) 69–77.
- [17] L. Upadhyaya, J. Singh, V. Agarwal, R.P. Tewari, The implications of recent advances in carboxymethyl chitosan based targeted drug delivery and tissue engineering applications, *J. Control. Release* 186 (2014) 54–87.
- [18] D. Mishra, B. Bhunia, I. Banerjee, P. Datta, S. Dhara, T.K. Maiti, Enzymatically crosslinked carboxymethyl-chitosan/gelatin/nano-hydroxyapatite injectable gels for in situ bone tissue engineering application, *Mater. Sci. Eng. C* 31 (2011) 1295–1304.
- [19] Z. Naghizadeh, A. Karkhaneh, A. Khojasteh, Simultaneous release of melatonin and methylprednisolone from an injectable in situ self-crosslinked hydrogel/microparticle system for cartilage tissue engineering, *J. Biomed. Mater. Res. A* 106 (2018) 1932–1940.
- [20] G. Wang, G.Y. Lu, Q. Ao, Y.D. Gong, X.F. Zhang, Preparation of cross-linked carboxymethyl chitosan for repairing sciatic nerve injury in rats, *Biotechnol. Lett.* 32 (2010) 59–66.
- [21] F. Schortgen, N. Deye, L. Brochard, C.S. Grp, Preferred plasma volume expanders for critically ill patients: results of an international survey, *Intensive Care Med.* 30 (2004) 2222–2229.
- [22] M. Raiman, C.G. Mitchell, B.M. Biccand, R.N. Rodseth, Comparison of hydroxyethyl starch colloids with crystalloids for surgical patients a systematic review and meta-analysis, *Eur. J. Anaesthesiol.* 33 (2016) 42–48.
- [23] C.M. Paleos, Z. Sideratou, D. Tsiourvas, Drug delivery systems based on hydroxyethyl starch, *Bioconjug. Chem.* 28 (2017) 1611–1624.
- [24] E. Kenawy, E.A. Kamoun, M.S.M. Eldin, M.A. El-Meligy, Physically crosslinked poly(vinyl alcohol)-hydroxyethyl starch blend hydrogel membranes: synthesis and characterization for biomedical applications, *Arab. J. Chem.* 7 (2014) 372–380.
- [25] J.F. Pan, H.F. Yuan, C.A. Guo, J. Liu, X.H. Geng, T. Fei, et al., One-step cross-linked injectable hydrogels with tunable properties for space-filling scaffolds in tissue engineering, *RSC Adv.* 5 (2015) 40820–40830.
- [26] J.F. Pan, L. Yuan, C.A. Guo, X.H. Geng, T. Fei, W.S. Fan, et al., Fabrication of modified dextran-gelatin in situ forming hydrogel and application in cartilage tissue engineering, *J. Mater. Chem. B* 2 (2014) 8346–8360.
- [27] L. Yuan, Y. Wu, J. Fang, X.J. Wei, Q.S. Gu, H. El-Hamshary, et al., Modified alginate and gelatin cross-linked hydrogels for soft tissue adhesive, *Artif. Cell Nanomed. B* 45 (2017) 76–83.
- [28] K.A. Kristiansen, A. Potthast, B.E. Christensen, Periodate oxidation of polysaccharides for modification of chemical and physical properties, *Carbohydr. Res.* 345 (2010) 1264–1271.
- [29] R. Fields, The measurement of amino groups in proteins and peptides, *Biochem. J.* 124 (1971) 581–590.
- [30] Y. Xin, J.Y. Yuan, Schiff's base as a stimuli-responsive linker in polymer chemistry, *Polym. Chem.-Uk* 3 (2012) 3045–3055.
- [31] Y. Jia, J.B. Li, Molecular assembly of Schiff base interactions: construction and application, *Chem. Rev.* 115 (2015) 1597–1621.
- [32] K.Y. Lee, K.H. Bouhadir, D.J. Mooney, Degradation behavior of covalently cross-linked poly(aldehyde guluronate) hydrogels, *Macromolecules* 33 (2000) 97–101.
- [33] R. Jayakumar, M. Prabakaran, P.T.S. Kumar, S.V. Nair, H. Tamura, Biomaterials based on chitin and chitosan in wound dressing applications, *Biotechnol. Adv.* 29 (2011) 322–337.